Yang Yang (Orcid ID: 0000-0002-9008-5137)
Wang Hailong (Orcid ID: 0000-0002-1994-4402)
Wang Pinya (Orcid ID: 0000-0001-7034-7868)
Chen Lei (Orcid ID: 0000-0003-1409-8371)
Liao Hong (Orcid ID: 0000-0001-6628-1798)

Fast climate responses to aerosol emission reductions during the COVID-19 pandemic

Yang Yang[1*], Lili Ren[1], Huimin Li[1], Hailong Wang[2], Pinya Wang[1], Lei Chen[1], Xu Yue[1], Hong Liao[1]

[1]Jiangsu Key Laboratory of Atmospheric Environment Monitoring and Pollution Control, Jiangsu Collaborative Innovation Center of Atmospheric Environment and Equipment Technology, School of Environmental Science and Engineering, Nanjing University of Information Science and Technology, Nanjing, Jiangsu, China

[2]Atmospheric Sciences and Global Change Division, Pacific Northwest National Laboratory, Richland, Washington, USA

*Correspondence to yang.yang@nuist.edu.cn

This article has been accepted for publication and undergone full peer review but has not been through the copyediting, typesetting, pagination and proofreading process which may lead to differences between this version and the Version of Record. Please cite this article as doi: 10.1029/2020GL089788

©2020 American Geophysical Union. All rights reserved.

Abstract

The reduced human activities and associated decreases in aerosol emissions during the COVID-19 pandemic are expected to affect climate. Assuming emission changes during lockdown, back-to-work and post-lockdown stages of COVID-19, climate model simulations show a surface warming over continental regions of the Northern Hemisphere. In January–March, there was an anomalous warming of 0.05–0.15 K in eastern China, and the surface temperature increase was 0.04–0.07 K in Europe, eastern U.S. and South Asia in March–May. The longer the emission reductions undergo, the warmer the climate would become. The emission reductions explain the observed temperature increases of 10–40% over eastern China relative to 2019. A southward shift of the ITCZ is also seen in the simulations. This study provides an insight into the impact of COVID-19 pandemic on global and regional climate and implications for immediate actions to mitigate fast global warming.

Accepted Article

©2020 American Geophysical Union. All rights reserved.

1. Introduction

The abrupt outbreak of the coronavirus disease 2019 (COVID-19) emerged in Wuhan of China in December 2019 and has been spreading worldwide, which has caused hundreds of thousands of deaths (Lu et al., 2020; Dong et al., 2020). In order to control the rapid spread of the disease, many countries have taken dramatic measures. As the early epicenter of the pandemics, China implemented a nationwide lockdown in late January 2020 (Tian et al., 2020), which greatly reduced human activities and hence primary air pollutant emissions, especially those from motor vehicle traffic. For example, nitrogen dioxide over China was cut in half after the outbreak of COVID-19, compared to that before the 2020 Lunar New year (Liu et al., 2020).

As a possible side effect of this unprecedented COVID-19 outbreak, many studies have examined the impact of the dramatic emission reductions on regional air quality (e.g., Le et al., 2020; Li et al., 2020; Sharma et al., 2020; Huang et al., 2020). Sharma et al. (2020) reported that the $PM_{2.5}$ (particulate matter less than 2.5 μm in diameter) concentration decreased by 43% in India during the COVID-19 lockdown period compared to past four years. Based on satellite and ground-based observations and regional model simulations, Le et al. (2020) and Huang et al. (2020) found that the unexpected heavy haze occurred in northern China during the COVID-19 period was mainly due to the high humidity and enhanced atmospheric

©2020 American Geophysical Union. All rights reserved.

oxidizing capacity that promoted the heterogeneous chemical reactions of aerosols, in conjunction with stagnant air conditions.

Besides its environmental impact, aerosol has been recognized as a major factor in affecting global and regional climate as it influences the radiation budget of the earth directly by scattering and absorbing solar radiation and indirectly by altering cloud properties (Boucher et al., 2013; Yang et al., 2019). Through interactions with radiation and cloud, aerosols can change the spatial structure of the atmospheric temperature, affect convection and monsoon circulation, and thus modify the hydrological cycle (Rosenfeld et al. 2008; Li et al., 2016). For instance, sulfate, as an important light scattering aerosol, can cause surface cooling over local and remote regions (Navarro et al., 2016; Yang et al., 2017a, 2018a). Black carbon (BC) heats the atmosphere through absorbing solar radiation (Bond et al., 2013; Yang et al., 2017b) and influences the East Asian monsoon and frequency of the extreme ENSO events through thermodynamic and dynamic feedbacks (Lou et al., 2019a,b). BC can enhance the Arctic amplification when depositing on ice or snow surfaces (Qian et al., 2014; Sand et al., 2016).

Previous studies about the reduced human activities during the COVID-19 mostly focused on its impact on air quality. Very few studies have explored possible global climate responses to the aerosol emissions reductions under the COVID-19 condition. In this work, an analysis of the impacts of restricted emissions during COVID-19 on global and regional climate is conducted based on a global aerosol-

©2020 American Geophysical Union. All rights reserved.

Accepted Article

climate model. We evaluate changes in aerosol concentrations, radiative forcing and their impacts on the surface air temperature and precipitation due to fast climate responses under multiple COVID-19 emission control scenarios in 2020. Hence, we provide the first-of-its-kind global insight into the impact of COVID-19 lockdown on climate, which can be used to assess potential changes in air quality and climate in response to the reduction of air pollutant emissions.

2. Methods

To investigate the fast response of the global climate to aerosol emission reductions during the COVID-19 period, we performed simulations using the CAM5 (Community Atmosphere Model version 5) model. The fast response refers to the rapid climate adjustments, which occur on a time scale much fast than response of ocean (Boucher et al., 2013). Major aerosol species, including sulfate, BC, primary organic matter (POM), secondary organic aerosol (SOA), mineral dust, and sea salt, are treated in the three lognormal modes (i.e., Aitken, accumulation and coarse modes) in this study (Liu et al., 2012). Aerosol radiative effects, as well as the aerosol microphysical impacts on stratiform clouds, are explicitly represented in the model. Based on the default CAM5, a few aerosol-related schemes are modified to improve the model performance, including aerosol convective transport and wet deposition (Wang et al., 2013).

The CAM5 simulations are performed for year 2020 with 1.9° latitude by 2.5° longitude horizontal grids and 30 vertical layers. Baseline anthropogenic and open

©2020 American Geophysical Union. All rights reserved.

biomass burning emissions of aerosols and precursors are from the CMIP6 (the Coupled Model Intercomparison Project Phase 6) SSP (Shared Socioeconomic Pathways) 2-4.5 scenario. Considering the possible biases of CMIP6 emissions in China (Ren et al., 2020a), which do not fully take into account the emission reduction from recent China clean air policies, we replace CMIP6 anthropogenic emissions in China with the MEIC (Multi-resolution Emission Inventory of China) inventory (Zheng et al., 2018). The baseline global aerosol emissions are taken from year 2017. Since the temporary emission reductions due to COVID-19 is unlikely to last for several years to substantially change the ocean heat content, monthly sea surface temperature (SST) and sea ice concentrations (SIC) are prescribed for every model year to the present-day climatology (averaged over 1982–2001) to avoid slow climate responses. Solar radiation and greenhouse gas concentrations are fixed at present-day conditions as well. In order to better match the observational large-scale circulation patterns, wind fields from the sixth model layer above the surface (~887 hPa) to the top of the model atmosphere (~3.6 hPa) are nudged to the MERRA-2 (Modern-Era Retrospective Analysis for Research and Applications Version 2) reanalysis (Rienecker et al., 2011) with a relaxation timescale of 6 h from April 1st 2019 to March 31st 2020 repeatedly for every model year.

To characterize the temporal variation of aerosol emissions during the COVID-19 pandemic, we split the whole period into three stages:

©2020 American Geophysical Union. All rights reserved.

1. COVID-Lock, during which the public is required to stay at home, traffic emissions are significantly reduced and industrial enterprises shut down;

2. Back to Work, when some industrial enterprises are allowed to resume production and the road traffic gradually increases;

3. Post-Lock, when most activities return to normal levels.

Since the COVID-19 pandemic is still going on, three different scenarios are designed to represent the possible emission pathways in year 2020 (Table S1). Because the disease prevalence and requirements of the lockdown varied greatly across countries, we deal with emissions separately for East Asia and the rest of the world. East Asia, especially China, took actions first to contain the disease spread in January 2020 and started the back-to-work stage in April. In the three emission reduction scenarios (FAST, MID and SLOW), we set months of January–March, April–June, and July–December as the periods of COVID-Lock, Back to Work and Post-Lock, respectively. For the rest of the world, three emission reduction scenarios are designed with fast (COVID-Lock: March–May and Back to Work: June–July), medium (COVID-Lock: March–July and Back to Work: August–November), and slow (COVID-Lock starts in March and lasts for a whole year) prevention and control assuming different situation of epidemic control, and are used in FAST, MID and SLOW simulations, respectively. In addition to the three emission reduction simulations, a CTRL simulation with baseline emissions is also performed as the reference case.

©2020 American Geophysical Union. All rights reserved.

Regional anthropogenic emission reduction ratios in China during the COVID-Lock period are calculated based on the provincial emission reduction ratio in Huang et al. (2020) and shown in Table S2. The emission reduction ratios for the rest of East Asia and the rest of the world follow the averaged values of China. Monthly variations in SO_2 emission are shown in Fig. S1 as an example. Within the total amount of emissions reductions, the transport sector is reduced by 70% during the COVID-Lock period with the remaining emission reduction attributed to all other sectors. All simulations are integrated for six years with the first year treated as model spin-up. Due to the prescribed SST/SIC and wind nudging, the model reaches an equilibrium state in a very short time and shows a weak interannual variability compared to the coupled atmosphere-ocean simulations (Yang et al., 2019), given that the standard deviation of annual mean global surface temperature is less than 0.002 K (0.006 K over land) during the last five years in all simulations.

The CAM5 model performance in reproducing aerosol concentrations were evaluated in many previous studies (e.g., Yang et al., 2017a,b, 2018b,c, 2020; Fan et al., 2018). Generally, the model can well simulate aerosols in North America and Europe, but significantly underestimates aerosol concentrations in East Asia and remote regions. As documented in a companion study of this work, the observed changes in aerosol concentrations in different regions of the world between the COVID-19 period in 2020 and the same time period in 2019, as well as the weekly variations of aerosol concentrations in early months of 2020, can be explained by

©2020 American Geophysical Union. All rights reserved.

both emission reductions and changes in meteorological parameters, which is well simulated by the model (Ren et al., 2020b).

3. Results

3.1 Changes in aerosols and radiative forcings

During the COVID-19 pandemic in 2020, the emission reductions due to the less traffic on road and other human activities lead to less aerosol loading all over the world (Fig. S2), with the magnitude of decreases depending on the emission reduction scenarios. The annual mean column burden of total sulfate and carbonaceous aerosols decreases mostly over Asia with maximum reductions of 2~5 mg/m^2 due to the relatively high baseline aerosol concentration over this region. Europe and North America have aerosol loadings lowered by 0.2~1.0 mg/m^2 considering emission reductions during COVID-19, compared to those in CTRL simulation. With a longer duration of the suspension of civic and commercial activities, more reductions in aerosols would occur, along with the less anthropogenic pollutants emitted into the atmosphere.

The less aerosol loadings in the emission reduction simulations result in lower aerosol optical depth (AOD) (Fig. S3), which further change the radiative balance of the earth. The radiative forcing due to aerosol-radiation interactions (RF_{ari}) at the top of the atmosphere (TOA) show positive anomalies (i.e., more clear-sky radiation absorbed by the earth system) over most land areas including the polluted regions (e.g., East Asia and South Asia), as well as the developed regions (e.g., Europe and

©2020 American Geophysical Union. All rights reserved.

North America). Negative anomalies (less radiation) of RF_{ari} are found in North Africa and the Middle East because over these dust dominant regions scattering (absorbing) aerosols have a reduced (enhanced) radiative impact on the bright surface with a high albedo (Myhre et al., 2013). Over these regions, RF_{ari} and its anomaly are both positive. In the cases of weaker aerosol light extinction (i.e., COVID-19 emission scenarios compared to CTRL), more solar radiation reaches the land surface and less is trapped by the absorbing aerosols (e.g., BC) in the atmosphere between 20°S–60°N, with the maximum radiative flux changes of 1–4 W/m^2. Globally, the changes in annual mean RF_{ari} at the TOA, surface and in the atmosphere are respectively in a range of 0.02~0.06, 0.11~0.23 and –0.08~–0.18 W/m^2 in the emission reduction simulations relative to CTRL, with an increasing magnitude in the order of FAST, MID and SLOW.

Through aerosol-cloud interactions, aerosol emission reductions during COVID-19 in 2020 produce anomalies of annual global mean radiative forcing (RF_{aci}) of 0.06~0.16 W/m^2 at the TOA with statistically significant positive values mainly over land and downwind oceanic regions (Fig. S5). Changes in RF_{aci} between emission reduction simulations and CTRL allow more energy reaching the surface and less energy absorbed by the atmosphere between 60°S and 60°N. Over the Arctic (60°–90°N), more (less) radiative energy is absorbed in the atmosphere (at the surface) in the COVID-19 emission reductions simulations, with regional mean RF_{aci} anomalies of –0.09~–0.28 W/m^2 at the surface, which is due to a significant decrease in low-

©2020 American Geophysical Union. All rights reserved.

level cloud fraction and the associated impact on longwave radiation over the Arctic (Fig. S6). The decreases in low-level cloud and downwelling longwave radiation can lead to a cooler Arctic surface than normal in boreal winter (Fig. S7). When sunlight comes to the Arctic in boreal summer, the reduced low-level cloud reflects less shortwave radiation to space and, therefore, the increased shortwave radiative flux reaching the surface offsets the decrease in longwave radiative flux, leading to the negligible net change in the Arctic surface temperature during this season. A possible reason for the low-level cloud decrease is associated with the atmospheric warming below 700 hPa (Fig. S8), which reduces cloud formation in the lower atmosphere. The decrease in sulfate aerosol serving as cloud condensation nuclei may also contribute to the decrease in low-level clouds. The cooling at the Arctic surface due to the decreased low-level clouds can stabilize the lower boundary layer and further reduce the low-level cloud amount. The lower-tropospheric warming in the Arctic is likely attributed to the decrease in SO_2 emissions in the mid-latitude regions, which increases the temperature gradient between mid-latitude and the Arctic and enhances poleward heat transport (Ren et al., 2020a).

3.2 Fast climate responses to COVID-19 emission reductions

Figure 1 shows the spatial distribution and zonal mean of changes in annual mean surface air temperature due to the COVID-19 emission reductions. In spite of the weak global average increase of 0.01–0.02 K over land, surface temperature responses are relatively strong at regional scale. With the consideration of fast

©2020 American Geophysical Union. All rights reserved.

Accepted Article

responses to emission reductions in the climate system, statistically significant warming appears primarily over continents of the Northern Hemisphere, especially eastern China, South Asia, Europe and eastern United States. The maximum warming locates over 30–50°N, with zonal mean surface air temperature changes of 0.02–0.04 K (0.04–0.07 K over land). In the Arctic, due to the decrease in low-level clouds, near-surface air temperature decreases substantially while a strong elevated warming arises in the lower atmosphere (below 700 hPa) as mentioned and explained above. Although large uncertainties exist in the Arctic due to the strong internal variability, the three scenarios give statistically significant results that are consistent with the varying magnitude of emission reductions.

Recall that regional emissions are reduced according to the possible duration and prevalence of COVID-19 pandemic in different regions. Figure 2 summarizes the monthly surface temperature changes in emission reduction simulations compared to CTRL over regions (Fig. S9) where the warming signals are mostly significant. The seasonal variations of surface temperature anomalies basically follow the emission reductions during COVID-19 applied to the model simulations. From January to March, due to the regional lockdown and sharply reduced human activities caused by the COVID-19 outbreak, eastern China is warmer than usual by 0.05–0.15 K. During April–June, when businesses were reopened in eastern China and outdoor activities were gradually resumed, the anomalous warming becomes progressively weaker but are still larger than 0.05 K. After July, temperature comes back to normal

©2020 American Geophysical Union. All rights reserved.

in the FAST simulation, in which scenario the world is assumed to quickly recover from COVID-19. However, the temperature is still slightly higher than normal in eastern China when the emission reductions remain for the rest of the world in the SLOW simulation. Due to the insignificant aerosol radiative impact over high latitudes of East Asia, the temperature anomaly averaged over the whole East Asia does not show a downward trend during 2020 as in eastern China, although it still shows an anomalous warming throughout the year.

When the COVID-19 pandemic occurred all over the world in March–May, the air starts to warm up due to the fast climate responses to the emission reductions. Simulated surface air temperature is higher than normal by 0.04–0.06 K in Europe and eastern U.S., while South Asia is warmed by about 0.07 K during this time period. After June, different scenarios lead to different pathways of temperature responses. In general, longer duration of emission reductions would produce a warmer climate in the second half of year 2020.

Unlike the temperature response, precipitation changes locate mostly over the tropics between 20°S and 20°N (Fig. 3). Comparing to CTRL, all emission reduction simulations exhibit an obvious southward shift of the intertropical convergence zone (ITCZ), with convective precipitation reduced over north-of-the-equator and enhanced over the south, which is mostly attributed to changes in thermodynamic conditions for convective precipitation induced by the aerosol change (Fig. S10). It results from the hemispheric asymmetry in BC-induced instantaneous atmospheric

©2020 American Geophysical Union. All rights reserved.

heating that changes the cross-equatorial heat transport and, consequently, causes a fast precipitation response (Yang et al., 2019). Zhao and Suzuki (2019) found that an increase in BC caused a northward shift of ITCZ shown as a fast precipitation response, which is consistent with our finding that a decrease in BC during COVID-19 leads to the southward shift of ITCZ. They also reported that increases in sulfate could change the tropical precipitation mainly through slow responses. This explains the weak impact of scattering aerosols on the tropical precipitation during the COVID-19 period with slow climate responses excluded from our simulations.

An important implication of the fast climate responses to the COVID-19 emission reductions is the impact on temperature in the real world. The year 2019 is reported as the second hottest year in terms of global and annual mean in the 140-year climate record (Lindsey, 2020). Based on data from NOAA/NCEI (National Oceanic and Atmospheric Administration/National Centers for Environmental Information), global mean surface temperature in the first three months of 2019 is 0.6 K higher than the 1971-2000 climatology (Fig. S11). In January–March of 2020, the observed global mean surface temperature is even higher than 2019 by 0.19 K. Over central and eastern China where aerosol emissions were substantially reduced due to the COVID-19 lockdown, observed temperature also increased. According to our simulations, in the first three months of 2020, COVID-19 related aerosol emission reductions can explain the temperature increases in 2020, compared to 2019, by 20–40% over the North China Plain, 10–20% over the Yangtze River Delta, 40–60%

©2020 American Geophysical Union. All rights reserved.

Accepted Article

over the Pearl River Delta and 10–40% over the Sichuan Basin (Fig. 4), which have been the top four most polluted regions in China.

4. Conclusions and Discussions

This study examines the fast climate responses to reduced aerosol emissions during the COVID-19 pandemic in 2020 based on a variety of aerosol-climate model simulations together with observations. By assuming emission reductions during three stages of the COVID-19 (i.e., COVID-Lock, Back to Work and Post-Lock) separately for East Asia and other regions of the world, three emission reduction scenarios are constructed in consideration of fast, medium, and slow prevention and control of the disease. The three scenarios show similar spatial patterns of global climate responses, but with different magnitudes, comparing to the baseline simulation without emission reductions. Surface warming appears primarily over land of the Northern Hemisphere with a zonal mean temperature increase of 0.04–0.07 K between 30 and 50°N, while the Arctic shows a near-surface cooling and lower tropospheric warming due to decreases in low-level cloud amount. During the COVID-Lock in January–March, eastern China is warmer than usual by 0.05–0.15 K. Surface air temperature is higher than normal by 0.04–0.07 K in Europe, eastern U.S. and South Asia in March–May. In the second half of year 2020, a longer duration of global emission reductions would produce a warmer climate. In the first three months of 2020, COVID-19 related aerosol emission reductions can explain the observed temperature increases in 2020 (relative to 2019) by 20–40% over the

©2020 American Geophysical Union. All rights reserved.

Accepted Article

North China Plain, 10–20% over the Yangtze River Delta, 40–60% over the Pearl River Delta and 10–40% over the Sichuan Basin. We also found a southward shift of the ITCZ, demonstrated by the BC-induced fast precipitation response in the tropics. This study implies that immediate actions for controlling the COVID-19 spread are the urgent need to not only save lives and economy but also mitigate the fast global warming.

There are many uncertainties in this study. For example, the emission reduction ratios applied in the simulations are mostly based on assumptions since the COVID-19 pandemic is still occurring over many countries of the world at this moment. The emission reduction ratios for the rest of East Asia and the rest of the world followed the averaged values of China, which could also lead to the uncertainty in the results. The emissions from air traffic and international shipping did not substantial reduced in the simulations as the transport sector with a reduction ratio of 70%. The impacts from these emission reductions need further study. Because simulated aerosol concentrations in China are underestimated in CAM5 and the nitrate and ammonium aerosols are not treated in the model, the climate responses to aerosols in China could be underestimated. Greenhouse gas emissions were also reduced during the COVID-19 confinement (Le Quéré et al., 2020), but the effects of reductions in greenhouse gases were not considered in this study. Only fast climate responses were examined, the COVID-19 emission reductions may also influence climate through slow oceanic processes and air-sea interactions if the emission reductions

©2020 American Geophysical Union. All rights reserved.

Accepted Article

would last for several years. In this study, wind fields above the planetary boundary layer were nudged to the MERRA-2 reanalysis, which could inhibit the potential impact of aerosol-induced circulation change on regional temperature distributions, although the significance of such an impact is questionable. While only one model is used in this study, the potential model dependence of climate responses to aerosol reductions warrants a further investigation using multi-model ensemble simulations. The Arctic shows very different climate response from that over mid-latitude regions, which requires more in-depth study with a consideration of the complex dynamic and thermodynamic processes and feedbacks as well as the availability of observations for the entire year 2020. Nevertheless, this study provides the first-of-its-kind insight into the impact of COVID-19 pandemic on global and regional climate, which can contribute to an assessment of the potential climate change in response to future reductions of air pollutant emissions.

Accepted Article

©2020 American Geophysical Union. All rights reserved.

Acknowledgments.

This research was support by the National Key Research and Development Program of China (grant 2019YFA0606800), the National Natural Science Foundation of China (grant 41975159) and Jiangsu Collaborative Innovation Center of Atmospheric Environment and Equipment Technology (special funding about meteorological impacts on virus spreading). We thank the Nanjing ZTweather technology Co., Ltd for providing data used for model evaluation. H. Wang was supported by the U.S. Department of Energy (DOE), Office of Science, Office of Biological and Environmental Research (BER), Earth and Environmental System Modeling (EESM) program. The Pacific Northwest National Laboratory (PNNL) is operated for DOE by Battelle Memorial Institute under contract DE-AC05-76RLO1830. Model results are available at https://zenodo.org/record/4023357.

Accepted Article

©2020 American Geophysical Union. All rights reserved.

References

Bond, T. C., Doherty, S. J., Fahey, D. W., Forster, P. M., Berntsen, T., DeAngelo, B. J., et al. (2013). Bounding the role of black carbon in the climate system: A scientific assessment. *Journal of Geophysical Research, 118,* 5380–5552. https://doi.org/10.1002/jgrd.50171.

Boucher, O., Randall, D., Artaxo, P., Bretherton, C., Feingold, G., Forster, P., et al. (2013). Clouds and Aerosols, in: Climate Change 2013: The Physical Science Basis, Contribution of Working Group I to the Fifth Assessment Report of the Intergovernmental Panel on Climate Change, edited by: Stocker, T. F., Qin, D., Plattner, G.-K., Tignor, M., Allen, S. K., Boschung, J., Nauels, A., Xia, Y., Bex, V., and Midgley, P. M., Cambridge University Press, Cambridge, UK and New York, NY, USA, 571–658, https://doi.org/10.1017/CBO9781107415324.016.

Dong, E., Du, H., & Gardner, L. (2020). An interactive web-based dashboard to track COVID-19 in real time. *Lancet Infectious Diseases, 20*, 533–534. https://doi.org/10.1016/S1473-3099(20)30120-1.

Fan, T., Liu, X., Ma, P.-L., Zhang, Q., Li, Z., Jiang, Y., et al. (2018). Emission or atmospheric processes? An attempt to attribute the source of large bias of aerosols in eastern China simulated by global climate models. *Atmospheric Chemistry and Physics*, *18*, 1395–1417. https://doi.org/10.5194/acp-18-1395-2018.

Huang, X., Ding, A., Gao, J., Zheng, B., Zhou, D., Qi, X., et al. (2020). Enhanced secondary pollution offset reduction of primary emissions during COVID-19 lockdown in China. *National Science Review*, nwaa137. https://doi.org/10.1093/nsr/nwaa137.

Le, T., Wang, Y., Liu, L., Yang, J., Yung, Y. L., Li, G., & Seinfeld, J. H. (2020). Unexpected air pollution with marked emission reductions during the COVID-19 outbreak in China. *Science*, eabb7431. https://doi.org/10.1126/science.abb7431.

Le Quéré, C., Jackson, R. B., Jones, M. W., Smith, A. J. P., Abernethy, S., Andrew, R. M., De-Gol, A. J., et al. (2020). Temporary reduction in daily global CO_2 emissions during the COVID-19 forced confinement. *Nature Climate Change*, 10, 647–653. https://doi.org/10.1038/s41558-020-0797-x.

Lindsey, R., (2019). was second-warmest year on record, https://www.climate.gov/news-features/featured-images/2019-was-second-warmest-year-record, last access: 05 July 2020.

©2020 American Geophysical Union. All rights reserved.

Li, L., Li, Q., Huang, L., Wang, Q., Zhu, A. S., Xu, J., et al. (2020). Air quality changes during the COVID-19 lockdown over the Yangtze River Delta Region: An insight into the impact of human activity pattern changes on air pollution variation. *Science of The Total Environment, 732*, 139282. https://doi.org/10.1016/j.scitotenv.2020.139282.

Li, Z., Lau, W. K.-M., Ramanathan, V., Wu, G., Ding, Y., Manoj, M. G., et al. (2016). Aerosol and monsoon climate interactions over Asia. *Reviews of Geophysics*, 119–161. https://doi.org/10.1002/2015RG000500.

Liu, F., Page, A., Strode, S. A., Yoshida, Y., Choi, S., Zheng, B., et al. (2020). Abrupt decline in tropospheric nitrogen dioxide over China after the outbreak of COVID-19. *Advancement of Science*, eabc2992. https://doi.org/10.1126/sciadv.abc2992.

Liu, X., Easter, R. C., Ghan, S. J., Zaveri, R., Rasch, P., Shi, X., et al. (2012). Toward a minimal representation of aerosols in climate models: description and evaluation in the Community Atmosphere Model CAM5. *Geoscientific Model Development, 5*, 709–739. https://doi.org/10.5194/gmd-5-709-2012.

Lou, S., Yang, Y., Wang, H., Lu, J., Smith, S. J., Liu, F., & Rasch P. J. (2019a). Black carbon increases frequency of extreme ENSO events. *Journal of Climate, 32*, 8323–8333. https://doi.org/10.1175/JCLI- D-19-0549.1.

Lou, S., Yang, Y., Wang, H., Smith, S. J., Qian, Y., & Rasch, P. J. (2019b). Black carbon amplifies haze over the North China Plain by weakening the East Asian winter monsoon. *Geophysical Research Letters, 46*, 452–460. https://doi.org/10.1029/2018GL080941.

Lu, R., Zhao, X., Li, J., Niu, P. H., Yang, B., Wu, H. L., et al. (2020). Genomic Characterization and Epidemiology of 2019 Novel Coronavirus: Implications for Virus Origins and Receptor Binding, *Lancet, 395*, 565-574. https://doi.org/10.1016/S0140-6736(20)30251-8.

Myhre, G., Myhre, C. E. L., Samset, B. H., & Storelvmo, T. (2013). Aerosols and their Relation to Global Climate and Climate Sensitivity, *Nature Education Knowledge 4*(5), 7.

Navarro, J. C. A., Varma, V., Riipinen, I., Seland, Ø., Kirkevåg, A., Struthers, H., et al. (2016). Amplification of Arctic warming by past air pollution reductions in Europe. *Nature Geoscience, 9*, 277–281. https://doi.org/10.1038/ngeo2673.

©2020 American Geophysical Union. All rights reserved.

Qian, Y., Wang, H., Zhang, R., Flanner, M. G., & Rasch, P. J. (2014). A sensitivity study on modeling black carbon in snow and its radiative forcing over the Arctic and Northern China. *Environmental Research Letters, 9*, 064001. https://doi.org/10.1088/1748-9326/9/6/064001.

Ren, L., Yang, Y., Wang, H., Zhang, R., Wang, P., & Liao, H. (2020a). Source attribution of Arctic aerosols and associated Arctic warming trend during 1980–2018. *Atmospheric Chemistry and Physics*. https://doi.org/10.5194/acp-2020-3, accepted.

Ren, L., Yang, Y., Wang, H., Wang, P., & Liao, H. (2020b). Aerosol transport pathways and source attribution in China during the COVID-19. in preparation.

Rienecker, M. M., Suarez, M. J., Gelaro, R., Todling, R., Bacmeister, J., Liu, R., et al. (2011). MERRA: NASA's Modern-Era Retrospective Analysis for Research and Applications. *Journal of Climate*, *24,* 3624–3648. https://doi.org/10.1175/JCLI-D-11-00015.1.

Rosenfeld, D., Lohmann, U., Raga, G. B., O'Dowd, C. D., Kulmala, M., Fuzzi, S., et al. (2008). Flood or drought: How do aerosols affect precipitation?. *Science, 321*(5894), 1309–1313. https://doi.org/10.1126/science.1160606.

Sand, M., Berntsen, T. K., von Salzen, K., Flanner, M. G., Langner, J., & Victor, D. G. (2016). Response of Arctic temperature to changes in emissions of short-lived climate forcers. *Nature Climate Change, 6*, 286–289. https://doi.org/10.1038/nclimate2880.

Sharma, S., Zhang, M., Anshika, Gao, J., & Kota, S. H. (2020). Effect of restricted emissions during covid-19 on air quality in india. *Science of The Total Environment, 728,* 138878. https://doi.org/10.1016/j.scitotenv.2020.138878.

Tian, H., Liu, Y., Li, Y., Wu, C., Chen, B., Kraemer, M. U. G., et al. (2020). An investigation of transmission control measures during the first 50 days of the COVID-19 epidemic in China. *Science, 368*, 638-642. https://doi.org/10.1126/science.abb6105.

Wang, H., Easter, R. C., Rasch, P. J., Wang, M., Liu, X., Ghan, S. J., et al. (2013). Sensitivity of remote aerosol distributions to representation of cloud-aerosol interactions in a global climate model. *Geoscientific Model Development, 6*, 765–782. https://doi.org/10.5194/gmd-6-765-2013.

©2020 American Geophysical Union. All rights reserved.

Yang, Y., Wang, H., Smith, S. J., Easter, R., Ma, P.-L., Qian, Y., et al. (2017a). Global source attribution of sulfate concentration and direct and indirect radiative forcing. *Atmospheric Chemistry and Physics*, *17*, 8903–8922. https://doi.org/10.5194/acp-17-8903-2017.

Yang, Y., Wang, H., Smith, S. J., Ma, P.-L., & Rasch, P. J. (2017b). Source attribution of black carbon and its direct radiative forcing in China. *Atmospheric Chemistry and Physics*, *17*, 4319–4336. https://doi.org/10.5194/acp-17-4319-2017.

Yang, Y., Wang, H., Smith, S. J., Easter, R. C., & Rasch, P. J. (2018a). Sulfate aerosol in the Arctic: Source attribution and radiative forcing. *Journal of Geophysical Research, 123*, 1899-1918. https://doi.org/10.1002/2017JD027298.

Yang, Y., Wang, H., Smith, S. J., Zhang, R., Lou, S., Yu, H., et al. (2018b). Source apportionments of aerosols and their direct radiative forcing and long-term trends over continental United States. *Earth's Future, 6*, 793–808. https://doi.org/10.1029/2018EF000859.

Yang, Y., Wang, H., Smith, S. J., Zhang, R., Lou, S., Qian Y., et al. (2018c). Recent intensification of winter haze in China linked to foreign emissions and meteorology. *Scientific Reports., 8*, 2107. https://doi.org/10.1038/s41598-018-20437-7.

Yang, Y., Smith, S. J., Wang, H., Mills, C. M., & Rasch, P. J. (2019). Variability, timescales, and nonlinearity in climate responses to black carbon emissions. *Atmospheric Chemistry and Physics*, *19*, 2405–2420. https://doi.org/10.5194/acp-19-2405-2019.

Yang, Y., Lou, S., Wang, H., Wang, P., & Liao, H. (2020). Trends and source apportionment of aerosols in Europe during 1980–2018. *Atmospheric Chemistry and Physics*, *20*, 2579–2590. https://doi.org/10.5194/acp-20-2579-2020.

Zhao, S., & Suzuki, K. (2019). Differing impacts of black carbon and sulfate aerosols on global precipitation and the ITCZ location via atmosphere and ocean energy perturbations. *Journal of Climate, 32*, 5567–5582. https://doi.org/10.1175/JCLI-D-18-0616.1.

Zheng, B., Tong, D., Li, M., Liu, F., Hong, C., Geng, G., et al. (2018). Trends in China's anthropogenic emissions since 2010 as the consequence of clean air actions. *Atmospheric Chemistry and Physics*, *18*, 14095–14111. https://doi.org/10.5194/acp-18-14095-2018.

©2020 American Geophysical Union. All rights reserved.

Accepted Article

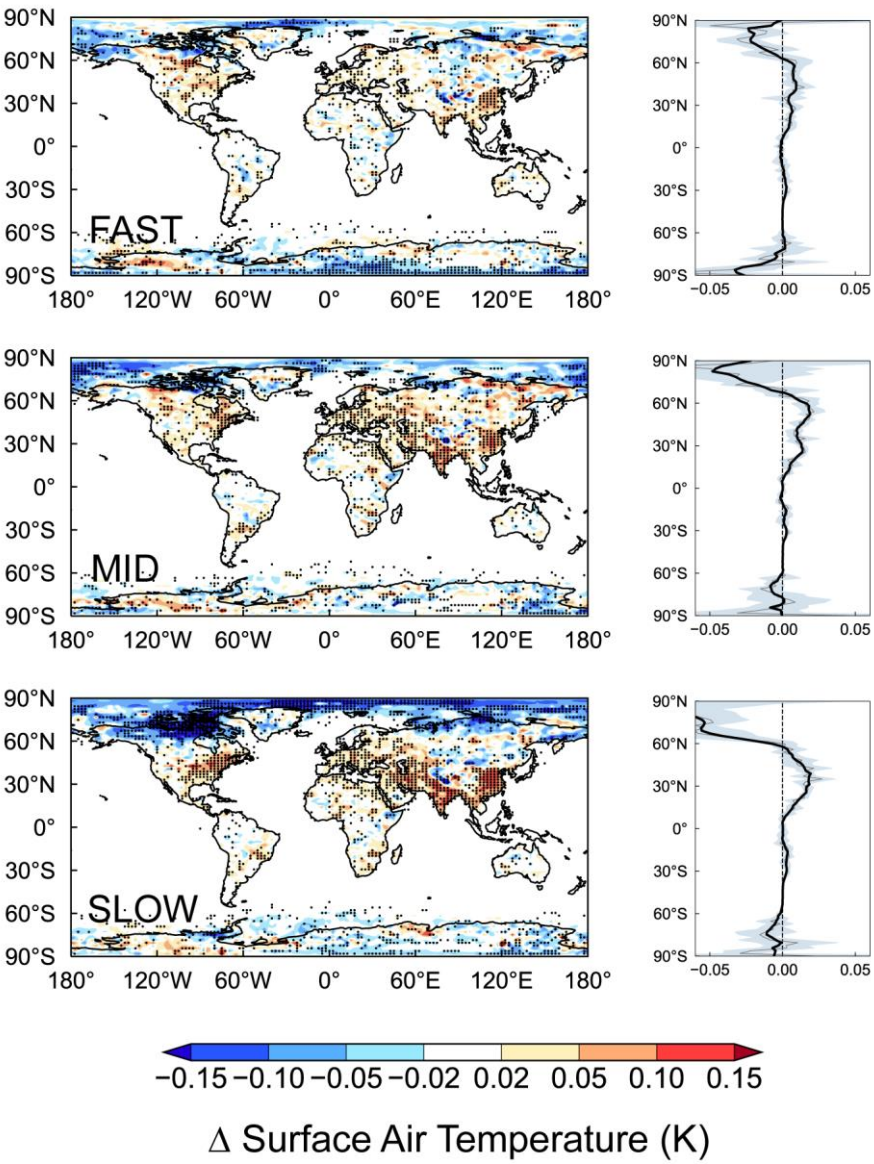

Figure 1. Spatial distribution (left) and zonal mean (right) of changes in annual mean surface air temperature (K) for FAST, MID and SLOW (from top to bottom) compared to CTRL. The stippled areas in left panels indicate statistical significance with changes larger than 1σ. Thin and thick black solid line in each right panel are zonal mean (with ±1σ denoted by the shaded area) and their 10° moving average.

©2020 American Geophysical Union. All rights reserved.

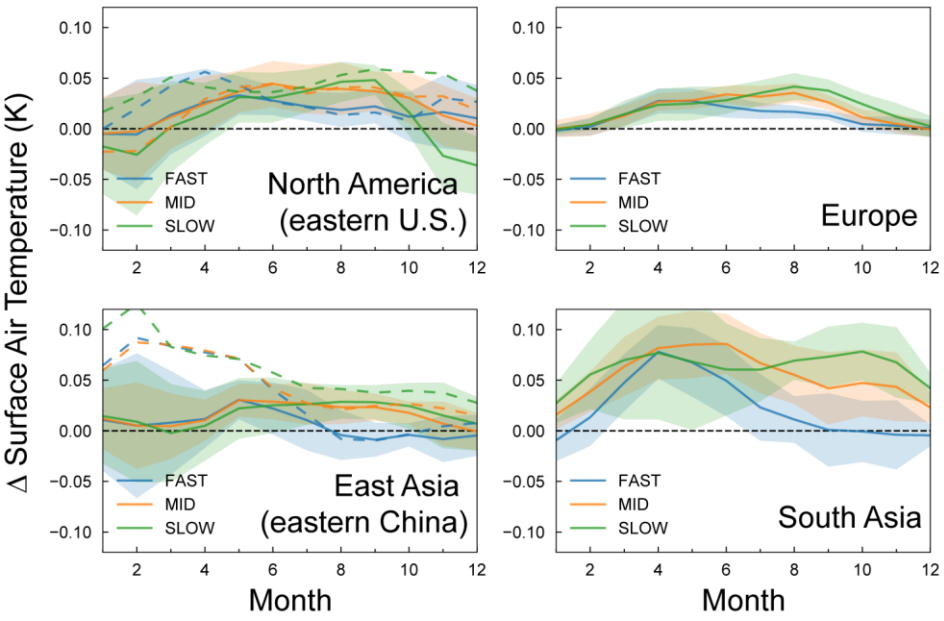

Figure 2. Changes in monthly mean surface air temperature (K) for FAST, MID and SLOW compared to CTRL averaged over North America (eastern U.S. in dashed lines), Europe, East Asia (eastern China in dashed lines) and South Asia. Regions are shown in Fig. S9. Shaded areas represent ±1σ.

Accepted Article

©2020 American Geophysical Union. All rights reserved.

Accepted Article

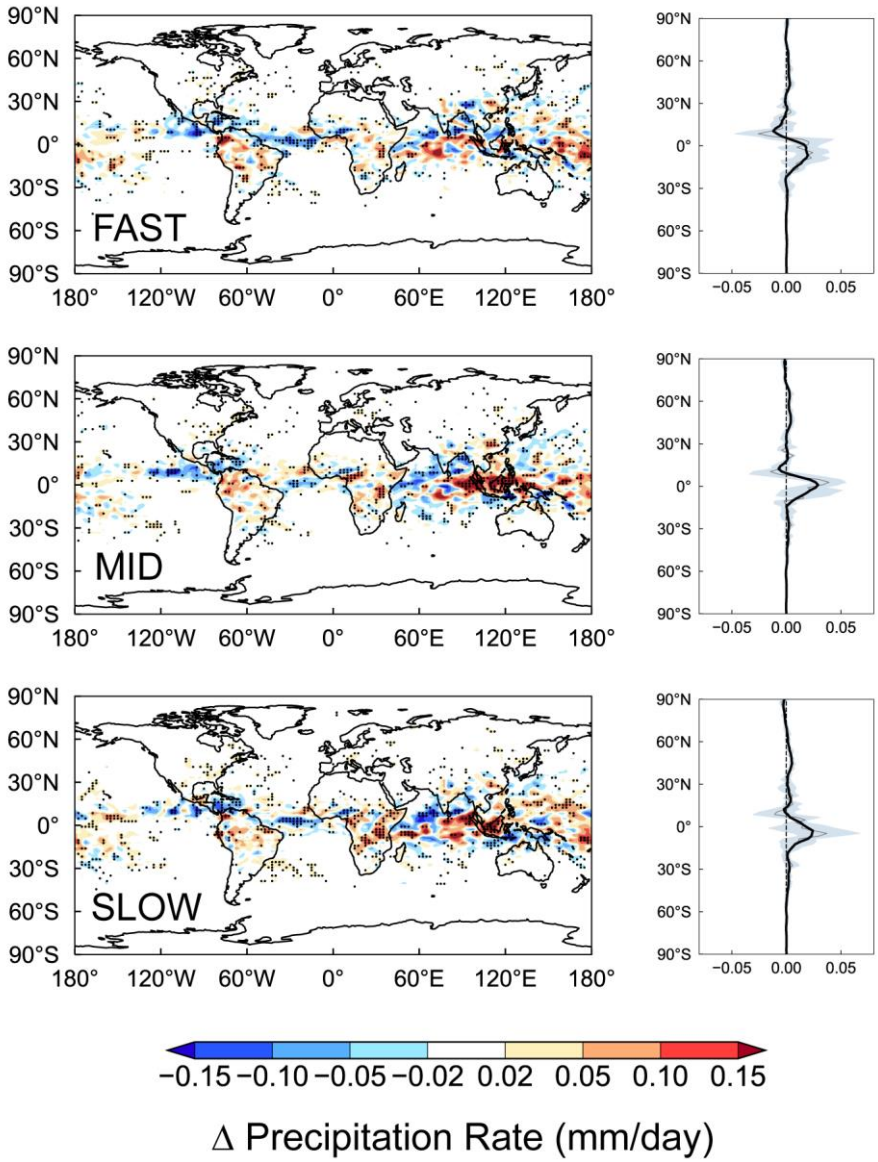

Figure 3. Spatial distribution (left) and zonal mean (right) of changes in annual mean precipitation rate (mm/day) for FAST, MID and SLOW (from top to bottom) compared to CTRL. The stippled areas in left panels indicate statistical significance with changes larger than 1σ. Thin and thick black solid line in each right panel are zonal mean (with ±1σ denoted by the shaded area) and their 10° moving average.

©2020 American Geophysical Union. All rights reserved.

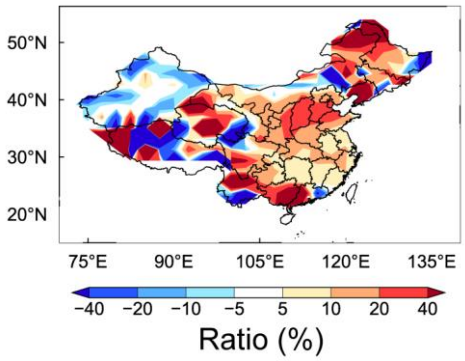

Figure 4. Ratio (%) of changes in January–March mean surface air temperature over China mainland due to the emissions reduction in the SLOW experiment relative to CTRL to the observed temperature difference between 2020 and 2019 from NOAA/NCEI, calculated as (SLOW–CTRL)/(Obs_2020–Obs_2019)×100%.

Accepted Article

©2020 American Geophysical Union. All rights reserved.